FERMILAB-CONF-08-360-E

Inclusive jet production at the Tevatron using the D0 experiment

Jeroen Hegeman on behalf of the D0 collaboration
Nikhef, PO Box 41882, 1009 DB Amsterdam, The Netherlands
The D0 experiment, Fermilab, PO Box 500-MS 357, Batavia, IL, 60510-0500, USA

E-mail: jhegeman@nikhef.nl

Abstract. A preliminary measurement is presented of the inclusive jet production cross section in $p\overline{p}$ collisions at a center-of-mass energy of $\sqrt{s}$ = 1960GeV. The data was taken with the D0 detector and represents an integrated luminosity of $\sim$ 900pb^{-1} of Tevatron RunII data. The cross section is studied as a function of jet transverse momentum (p_{T}) and rapidity (y) and compared to perturbative QCD predictions in next-to-leading order including two-loop threshold corrections.

1. Introduction

A broad range of physics can be studied in QCD jet production. Understanding high p_{T} jets can help constrain Parton Distribution Functions (PDFs) whereas soft jets allow one to study soft physics and hadronization. In addition, knowledge of multi-jet production and event topology is essential for the understanding of standard model backgrounds in the search for new physics. The inclusive jet production cross section is a fundamental property of QCD and directly comparable to perturbative QCD predictions.

2. Inclusive jet production cross section measurement

The cross section is measured in two central jet rapidity regions: $|y_{\mathrm{jet}}| < 0.4$ and $0.4 < |y_{\mathrm{jet}}| < 0.8$.

2.1. Jet energy calibration

The measured jet energies (E_{cal}) are calibrated to the particle level using the expression

$$E_{\mathrm{ptcl}} = \frac{E_{\mathrm{cal}} - O}{R \cdot S}$$

which corrects for offset energy O, jet response R and detector showering effects S. The offset is determined from zero-bias events and corrects for calorimeter noise, pile-up effects and the soft underlying event. The absolute response is determined by requiring p_{T} balance in photon+jet events. The photon energy scale is determined by calibrating the electromagnetic calorimeter on the $\mathrm{Z} \rightarrow \mathrm{e}^-\mathrm{e}^+$ peak and combining this with the relative electron-photon energy scale. The dependence of the response on detector pseudorapidity is determined using both photon+jet and di-jet events. Parts of the particle shower in the calorimeter may escape the jet cone. A net correction for this showering effect is derived by measuring the energy density profile around a

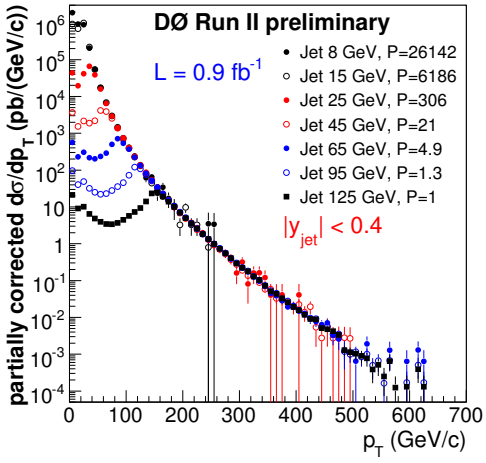

Figure 1. Partially corrected inclusive jet cross section in the central rapidity bin, measured with different jet triggers at different E_{T} thresholds.

jet and subtracting the energy leaving the jet cone due to physics effects estimated from Monte Carlo.

2.2. Jet p_T- and rapidity resolutions

The jet p_{T} resolution is measured on a subsample of the full dataset used for the analysis by looking at the p_{T} imbalance (A) in di-jet events

$$A = \frac{|p_{\mathrm{T},1} - p_{\mathrm{T},2}|}{p_{\mathrm{T},1} + p_{\mathrm{T},2}}$$

after corrections for soft radiation (which results in additional jets below the reconstruction threshold) and particle level imbalances.

The jet p_{T} spectra are fitted iteratively with a four-parameter Ansatz function

$$f(N, \alpha, \beta, \gamma) = N(p_{\mathrm{T}}/1\mathrm{GeV})^{-\alpha} \times \left(1 - \frac{2p_{\mathrm{T}}\cosh(y_{\mathrm{min}})}{\sqrt{s}}\right)^{\beta} \exp(-\gamma p_{\mathrm{T}})$$

convoluted with Gaussian resolutions determined from data. Here y_{min} is the lower rapidity limit of the bin, and $\sqrt{s}$ is the center-of-mass energy: $\sqrt{s} = 1960\mathrm{GeV}$.

The ratio of folded to original Ansatz function is used to unfold the data for resolution effects. Another method based on simulated Monte Carlo events generated with the PYTHIA [1] generator and smeared with the resolutions as obtained from data was used to cross-check this method and excellent agreement was obtained.

2.3. Results

Data from seven different single-jet triggers with different transverse energy thresholds was selected for this measurement (see Fig. 1). The different trigger samples are matched using the relative trigger efficiencies and corrected for both jet identification and event selection efficiency.

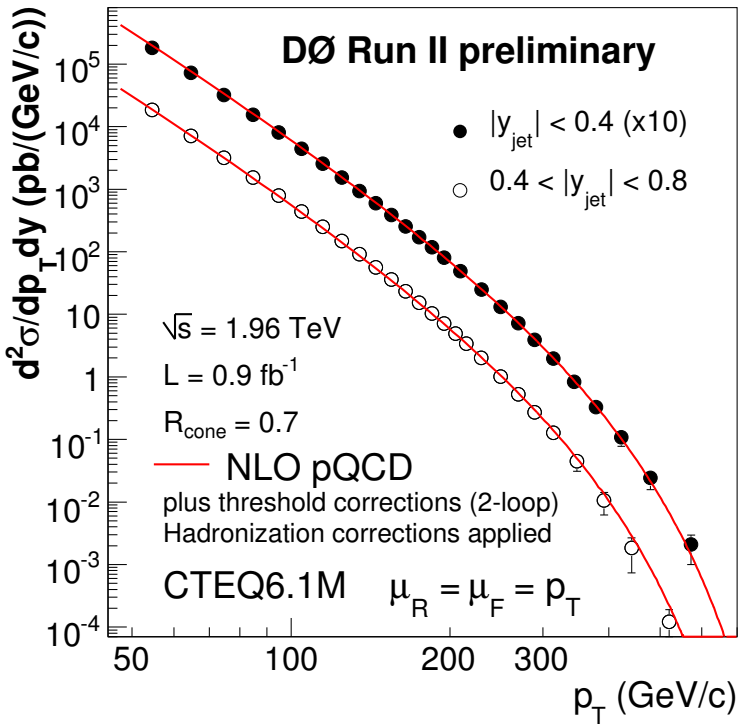

Figure 2. The inclusive jet cross section, measured in two regions of jet rapidity. Error bars show the total measurement uncertainty. The predicted curves from pQCD are corrected for hadronisation effects and are overlaid on the data.

2.4. Comparison to perturbative QCD

The measured cross section is compared to the prediction from next-to-leading order (NLO) theory including two-loop accuracy threshold corrections [2]. The NLO calculations were performed with NLOjet++ [3] and FastNLO [4]. Figure 3 shows the ratio of data to theory prediction for both rapidity bins. Also shown are the uncertainty on the CTEQ6.1M [5; 6] PDF (dashed lines) and the next-to-leading order theory prediction without threshold corrections (dash-dotted line). The different high-p_{T}behavior between the two rapidity bins is attributed to limited statistics in the jet energy calibration sample. Note that the measurement is becoming precise enough to start constraining the PDFs at high p_{T}. Since the uncertainty due to the PDFs is dominated by the uncertainty on the gluon PDF at high momentum fraction x, this mainly pertains to the gluon PDF.

Figure 4 shows the relative contributions of the different sources of uncertainty. It is obvious that a significant gain is to be obtained from a better calibration of the jet energy scale.

3. Conclusion

Preliminary results are presented on the inclusive jet cross section at D0. The results are in good agreement with next-to-leading order perturbative QCD. The measurement gains increasing sensitivity [7] to the gluon PDFs at high momentum transfers. This will be one of the leading uncertainties in searches beyond the standard model both at the Fermilab Tevatron collider and at the CERN proton-proton collider (LHC).

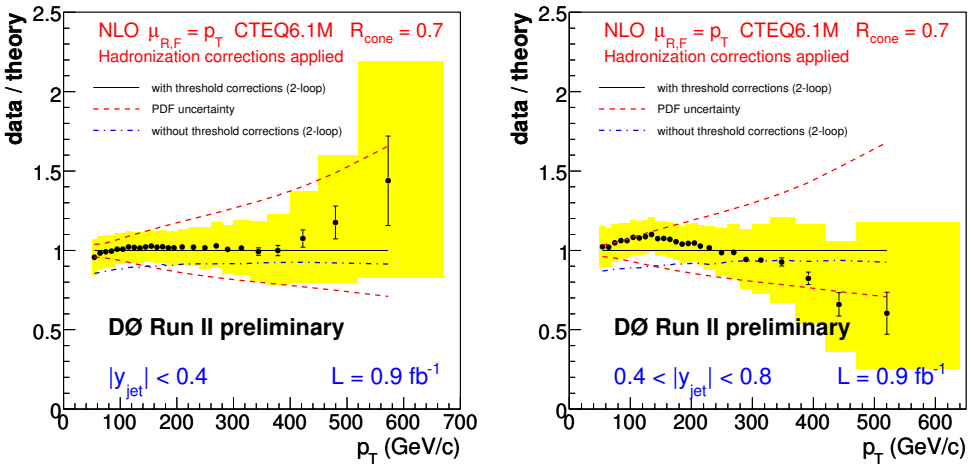

Figure 3. Inclusive jet cross section compared to the theory prediction, measured in two regions of jet rapidity. Error bars and band show statistical and systematic uncertainty, respectively.

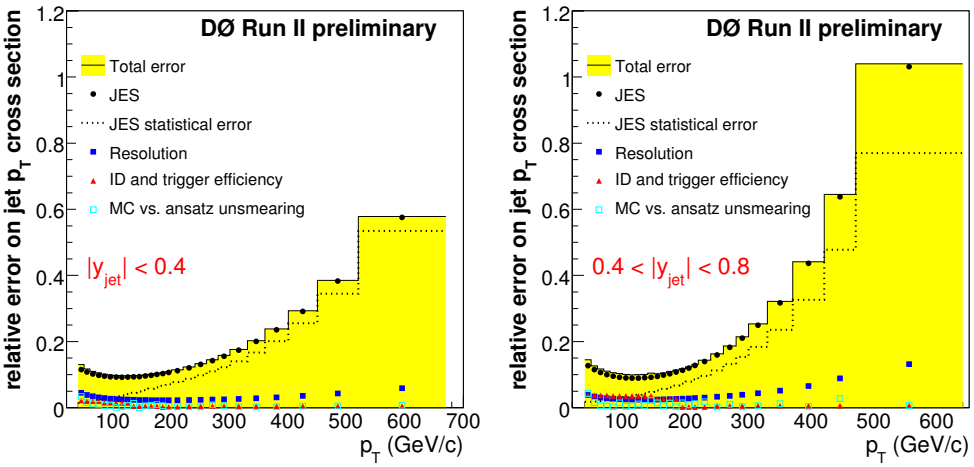

Figure 4. Contributions from different sources of uncertainties

References

[1] Sjostrand T *et al.* 2001 *Comput. Phys. Commun.* **135** 238–259 (*Preprint* `hep-ph/0010017`)

[2] Kidonakis N and Owens J F 2001 *Phys. Rev.* **D63** 054019 (*Preprint* `hep-ph/0007268`)

[3] Nagy Z 2003 *Phys. Rev.* **D68** 094002 (*Preprint* `hep-ph/0307268`)

[4] Kluge T, Rabbertz K and Wobisch M 2006 (*Preprint* `hep-ph/0609285`)

[5] Pumplin J *et al.* 2002 *JHEP* **07** 012 (*Preprint* `hep-ph/0201195`)

[6] Stump D *et al.* 2003 *JHEP* **10** 046 (*Preprint* `hep-ph/0303013`)

[7] Abbott B *et al.* (D0) 1999 *Phys. Rev. Lett.* **82** 2451–2456 (*Preprint* `hep-ex/9807018`)